Journal of Molecular Graphics and Modelling 34 (2012) 18–27

Contents lists available at SciVerse ScienceDirect

Journal of Molecular Graphics and Modelling

journal homepage: www.elsevier.com/locate/JMGM

Molecular modeling study on the possible polymers formed during the electropolymerization of 3-hydroxyphenylacetic acid

Deusmaque Carneiro Ferreira[a,b], Antonio Eduardo da Hora Machado[b,c], Fernanda de Souza Tiago[b], João Marcos Madurro[b], Ana Graci Brito Madurro[d], Odonírio Abrahão Jr.[a,*]

[a] Instituto de Ciências Biológicas e Naturais, Universidade Federal do Triângulo Mineiro, Praça Manoel Terra, 330, 38015-050, Uberaba, Minas Gerais, Brazil
[b] Instituto de Química, Universidade Federal de Uberlândia, Uberlândia, Minas Gerais, Brazil
[c] Departamento de Química, Universidade Federal de Goiás, Campus Catalão, Catalão, Goiás, Brazil
[d] Instituto de Genética e Bioquímica, Universidade Federal de Uberlândia, Uberlândia, Minas Gerais, Brazil

ARTICLE INFO

Article history:
Received 13 October 2011
Received in revised form
28 December 2011
Accepted 5 January 2012
Available online 14 January 2012

Keywords:
Conductive polymer
Electrochemical biosensors
RM1
DFT
Monte Carlo conformational analysis
Polymer structure
Reaction mechanism

ABSTRACT

The compound 3-hydroxyphenylacetic acid (3-HPA) has been used as a monomer in the synthesis of polymeric films by electropolymerization; these films serve as supports for the immobilization of biomolecules in electrochemical biosensors. To assist in the elucidation of the mechanism of 3-HPA electropolymerization, a systematic quantum mechanical study was conducted. In addition to the monomer, all possible intermediates and the probable oligomers formed during the electropolymerization were investigated using a density functional theory (DFT) method combined with a previous conformational analysis performed with the aid of the RM1 semi-empirical method or a Monte Carlo conformational analysis with the force field OPLS-2005. From the data analysis combined with the experimental results, a mechanism was proposed for the main route of formation of the polymeric films. The mechanism involves the formation of polyethers from the coupling of phenoxide radicals and radicals based on the aromatic ring.

1. Introduction

Conducting polymers are poly-conjugated structures whose electronic properties resemble those of metals while the compounds themselves retain the properties of conventional organic polymers [1]. This type of polymer has been highlighted because of its numerous applications, which include solar cells [2], batteries [3], electronic devices [4], sensors and biosensors [5].

In contrast, non-conducting polymers are insulating materials that show self-limited growth due to their high resistivity [6]. The diffusion of substrates and products on non-conducting polymers tend to be fast because of the polymers' low thickness, which typically ranges between 10 and 100 nm [7,8]. The fast diffusion kinetics of these polymers are useful in preventing contamination of electrode surfaces by interfering species and in the development of biosensors [5,9].

Electrodes based on conducting materials (glassy carbon, graphite, gold, and platinum, among others) can be chemically modified with conducting polymers or even non-conducting polymers to alter relevant surface properties, such as their electrical conductivity, reactivity and roughness [10]. Chemically modified electrodes stand out because of the optimization of selective interactions at their surfaces, their ability to pre-concentrate analytes in the modified layer, their ability to transfer electrons in the electrocatalysis of redox reactions, their ability to electrochemically detect ionic analytes and their ability to incorporate biomolecules [11].

Conducting or non-conducting polymers can be synthesized either chemically (condensation or addition polymerization) or electrochemically by oxidation of monomers on the working electrode, which forms radical cations that react with other monomers or radical cations to produce insoluble polymer chains on the electrode surface [12]. The most widely investigated polymers for the fabrication of modified electrodes include polyaniline, poly-(phenylenevinylene), polypyrrole and polythiophene [1]. In addition, electrodes chemically modified by functionalized polymers are excellent candidates for the development of biosensors because they are relatively cheap materials, the production techniques are simple, they can be deposited on various types of substrates, the thickness and homogeneity of the films are easily controlled, and the choice of different molecu-

* Corresponding author. Tel.: +55 34 3318 5487; fax: +55 34 3318 5462.
E-mail address: odonirio@biomedicina.uftm.edu.br (O. Abrahão Jr.).

1093-3263/$ – see front matter © 2012 Elsevier Inc. All rights reserved.
doi:10.1016/j.jmgm.2012.01.001

lar structures allows for the construction of films with different characteristics [13]. We have reported the in situ preparation of electrodes coated with several functionalized polymers applied in biosensors: polyaminophenols [14], polytyramine [15], poly-4-methoxyphenethylamine [16], poly-(4-hydroxybenzoic) acid [17], poly-(4-hydroxyphenylacetic) acid [18].

Recently, members of our group reported, for the first time in the literature, the electropolymerization of 3-hydroxyphenylacetic acid (3-HPA) onto a graphite electrode. The modified electrode presented well-defined redox peaks, which indicated the electrodeposition of an electroactive material. Incorporation experiments with oligonucleotides and hybridization with the complementary target indicated that this modified electrode is a promising device for the development of DNA biosensors [19]. An understanding of the mechanism of electropolymerization and the elucidation of the polymer structure are prerequisites for understanding its reactivity and interactions with biomolecules.

Given the rapid technological development of computer science, methods of computational chemistry have experienced unprecedented development and have been applied in molecular modeling, rational planning and the study of different compounds, including conducting and non-conducting polymers, synthesis mechanisms, complex interactions such as those involving bioactive compounds, etc. The application of molecular modeling enables a detailed description of the structure, the intermolecular interactions and, if applicable, the chemical reactions related to the production of polymers and others compounds used to functionalize the surface of the electrodes to efficiently promote the immobilization of biomolecules on the sensor surface [17,18].

Understanding of the intermolecular interactions between these polymeric films and molecules of biological interest that have been immobilized without alteration of their biological activities is essential to ensure the functionality of devices for quick analyses that are free of interfering species and that exhibit high sensitivity and selectivity. Thus, the aim of the present study is to contribute to the understanding of the intermolecular interactions between these polymeric films and molecules of biological interest by elucidating the mechanism of 3-HPA electropolymerization in an acidic medium using a combination of experimental and quantum mechanical methods.

2. Experimental methods

2.1. Calculations

Initially, 3-HPA was submitted to a systematic conformational analysis using the semi-empirical RM1 method [20] (AMPAC, version 9.2) to obtain the potential energy surface related to its two main free dihedral angles. The global minimum structure was optimized, and its vibration frequencies were calculated employing the method of density functional theory (DFT) using the hybrid functional B3LYP and the atomic basis sets 6-31G(d) for monomers and 6-31G(d,p) for the three polymer models. All DFT calculations were performed using Gaussian 09 [21].

The same calculations were applied without symmetry restrictions to the possible intermediates generated during the electropolymerization (Scheme 1); the intermediates were derived from the optimized structure of 3-HPA, with only the charge and multiplicity changed. Calculations to account for the influence of water as a solvent were also performed for each of these species according to the integral equation formalism of polarized continuum solvation method (IEFPCM) [22].

The minimum-energy geometries, energies and configurations of the *highest occupied molecular orbital* (HOMO), the *lowest unoccupied molecular orbital* (LUMO) for molecules with odd multiplicities, and alpha and beta *singly occupied molecular orbitals* (SOMO) for the even multiplicities were estimated from the results of the calculations. In addition to the frontier molecular orbital, the partial atomic charges and their variations for each intermediate studied were analyzed using the ChelpG method [23,24]. Changes in the chemical bonds issued by variations in bond orders were analyzed with the natural bonding orbitals (NBO) method in an unrestricted DFT calculation using the 6-31G(d) atomic basis set to describe all atoms [21,22]. Changes in the electronic energies, ionization energies, dipole moments and electron density maps superimposed on the total potential energy surfaces were also evaluated. In addition, the PM6 semi-empirical model from MOPAC 2009 [25] was used to calculate the pKa_1 and pKa_2 of 3-HPA for comparison with experimental measurements. The experimental values of p*Ka* were determined by acid–base titration using a standard solution of 0.935 mol L^{-1} NaOH; the titration results were treated using the program CurTiPot® 3.2.

Possible dimeric structures were modeled and submitted to scans of the main dihedral angles with the OPLS 2005 and AMBER force fields [26]. With these models, the quality of the parameters to simulate the structures of films formed from 3-HPA in these force fields can be evaluated by observation of the torsional energy barriers compared to equivalent scans obtained from DFT calculations. From these analyses, the OPLS force field was selected for conformational analyses of the studied oligomers. These analyses were only possible with additional torsional parameters available in the Macromodel software [26].

Three possible octamers were designed and submitted to conformational searching by the application of the Monte Carlo multiple minimum (MCMM) stochastic method. The conformers were analyzed and grouped according to energy and structure. After each search, the redundant conformers were eliminated, which facilitated the sampling results. A cut-off of 0.5 Å for

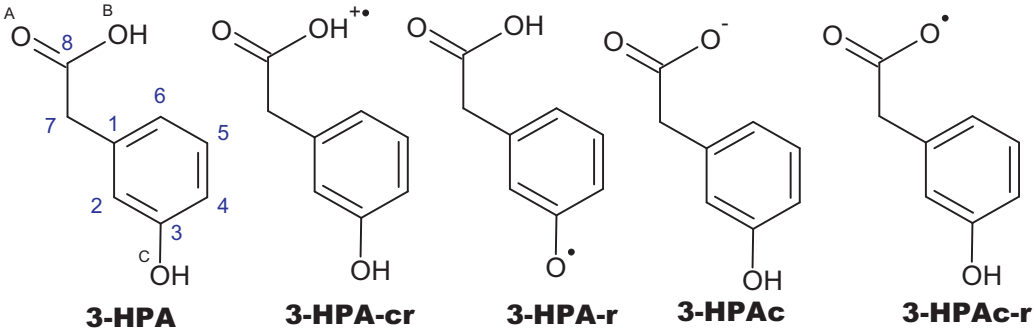

Scheme 1. Representation of the 3-hydroxyphenylacetic acid (3-HPA); the numbering is adopted for the atoms in all calculations of this work and in possible intermediates formed during the electropolymerization: 3-hydroxyphenylacetic acid cation radical (3-HPA-cr), 3-hydroxyphenyl acetic acid radical (3-HPA-r), 3-hydroxyphenyl acetate (3-HPAc), and 3-hydroxyphenyl acetate radical (3-HPAc-r).

Table 1
Selected geometric parameters (bond lengths, angles and dihedrals) obtained using DFT calculations for 3-HPA and intermediates produced during the electropolymerization.

Interactions	3HPA	3HPA-cr	3HPA-r	3HPAc	3HPAc-r
C1–C2	1.405	1.391	1.395	1.391	1.391
C1–C7	1.524	1.494	1.519	1.493	1.494
O(c)–H	0.984	0.960	–	0.963	0.964
C8–O(A)	1.220	1.219	1.205	1.218	1.219
C8–O(B)	1.344	1.348	1.353	1.350	1.348
O(B)–H	0.989	0.960	0.968	–	–
C2–C3–O(C)	122.6	123.1	122.2	123.1	123.1
C4–C3–O(C)	117.2	115.2	117.3	115.1	115.2
H–C7–H	106.4	104.6	108.8	104.8	104.6
C7–C8–O(A)	124.1	127.2	125.1	127.7	127.2
C7–C8–O(B)	112.0	113.1	112.2	112.7	113.1
O(a)–C8–O(B)	123.7	119.5	122.5	119.4	119.5
C8–O(B)–H	107.5	109.4	106.9	–	–
C6–C1–C7–C8	122.1	110.0	115.6	106.5	110.0
C1–C7–C8–O(A)	−65.8	70.0	86.2	−99.9	70.0
C1–C7–C8–O(B)	110.9	−109.7	−92.5	80.0	−109.7
H–C7–C8–O(B)	−127.7	14.1	29.1	−157.1	14.1

the maximum distance between corresponding atoms after superimposition was used to distinguish the conformers that were being generated in each method.

The global-minimum-energy conformers were submitted to calculations using the semi-empirical model RM1 [25] to pre-optimize the structures for the calculation of vibrational frequencies. These structures were re-optimized, and the infrared spectra were simulated using the B3LYP hybrid functional and the 6-31G(2d,p) atomic basis set. The infrared spectra were also simulated for comparison purposes using the semi-empirical model RM1 based on MOPAC 2009. The Gabedit graphical interface was used to visualize the results [27]. In both situations, the most intense vibration modes were compared to experimental data to ascertain the structure of the octamer models that best represent the experimentally obtained polymer.

3. Results and discussion

The 3-HPA is an electrochemically active compound that contains two functional groups in its chemical structure: a hydroxyl group (—OH) and an aceto group (—CH_2COOH). Scheme 1 shows the structure of 3-HPA and those of possible intermediates formed during the electropolymerization.

Fig. 1 presents the potential energy surfaces related to two of the principal free dihedral angles of 3-HPA (dihedrals C8–C7–C1–C6 and O(A)–C8–C7–C1) obtained by a systematic conformation analysis using RM1. The structure of the global minimum found from the potential energy surface was selected for DFT calculations.

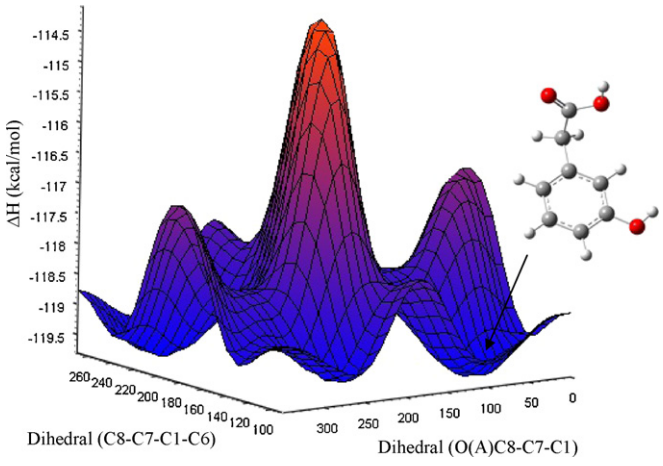

Fig. 1. Potential-energy surface for 3-HPA obtained by a systematic conformation analysis using the semi-empirical method RM1.

The geometric parameters for 3-HPA, 3-HPA-cr, 3-HPA-r, 3-HPAc, and 3-HPAc-r, which were selected from minimum-energy structures obtained by DFT calculations, are presented in Table 1.

The analysis of the geometric data shows a slight shortening of the C(1)–C(7) bond length for the studied intermediates compared to that in 3-HPA (Table 1). The bond order for this bond also increases (Table 2), as does the partial charge over carbon 7 in these intermediates (Fig. 2 and Scheme 1), except for that in the free radical 3-HPA-r.

Fig. 2a shows that the more negative partial charge in 3-HPA is over the oxygen of the OH in the carboxylic group, followed by the oxygen of the phenolic group. The partial charge over carbon 8 (see Scheme 1) is the most positive among the atomic partial charges in this molecule because of resonance in the carboxylic group. The next-highest positive charge is that of carbon 3, which is connected to the phenolic group. The strong negative partial charge on carbon 7 is probably a consequence of an inductive effect between the carboxylic group and the aromatic ring because, based on the analysis of the charge distribution over the intermediate 3-HPA-cr (Fig. 2b), which presents a partial charge distribution approximately similar to that calculated for 3-HPA, the partial charge over carbon 6 is

Table 2
Bond orders for 3-HPA and intermediates produced during 3-HPA electropolymerization.

Interaction	3HPA	3HPA-cr	3HPA-r	3HPAc	3HPAc-r
C1–C2	1.391	1.472	1.404	1.378	1.377
C1–C6	1.419	1.259	0.666	1.398	1.405
C1–C7	0.997	1.018	0.871	1.012	1.000
C2–C3	1.391	1.279	1.259	1.399	1.386
C2–H	0.914	0.883	0.709	0.893	0.905
C3–C4	1.347	1.181	1.369	1.344	1.343
C3–O(C)	1.025	1.162	1.280	1.003	1.032
C4–C5	1.464	1.525	1.422	1.450	1.460
C4–H	0.909	0.884	0.914	0.919	0.906
C5–C6	1.410	1.343	1.420	1.420	1.411
C5–H	0.914	0.889	0.867	0.924	0.912
C6–H	0.915	0.896	0.743	0.918	0.913
O(C)–H	0.743	0.695	–	0.751	0.745
C7–C8	0.972	0.949	0.932	0.923	0.962
C7–H	0.893	0.854	0.863	0.902	0.871
C7–H	0.895	0.888	0.910	0.915	0.895
C8–O(A)	1.765	1.811	1.723	1.579	1.676
C8–O(B)	1.049	1.020	1.037	1.364	1.161
O(B)–H	0.715	0.718	0.812	–	–

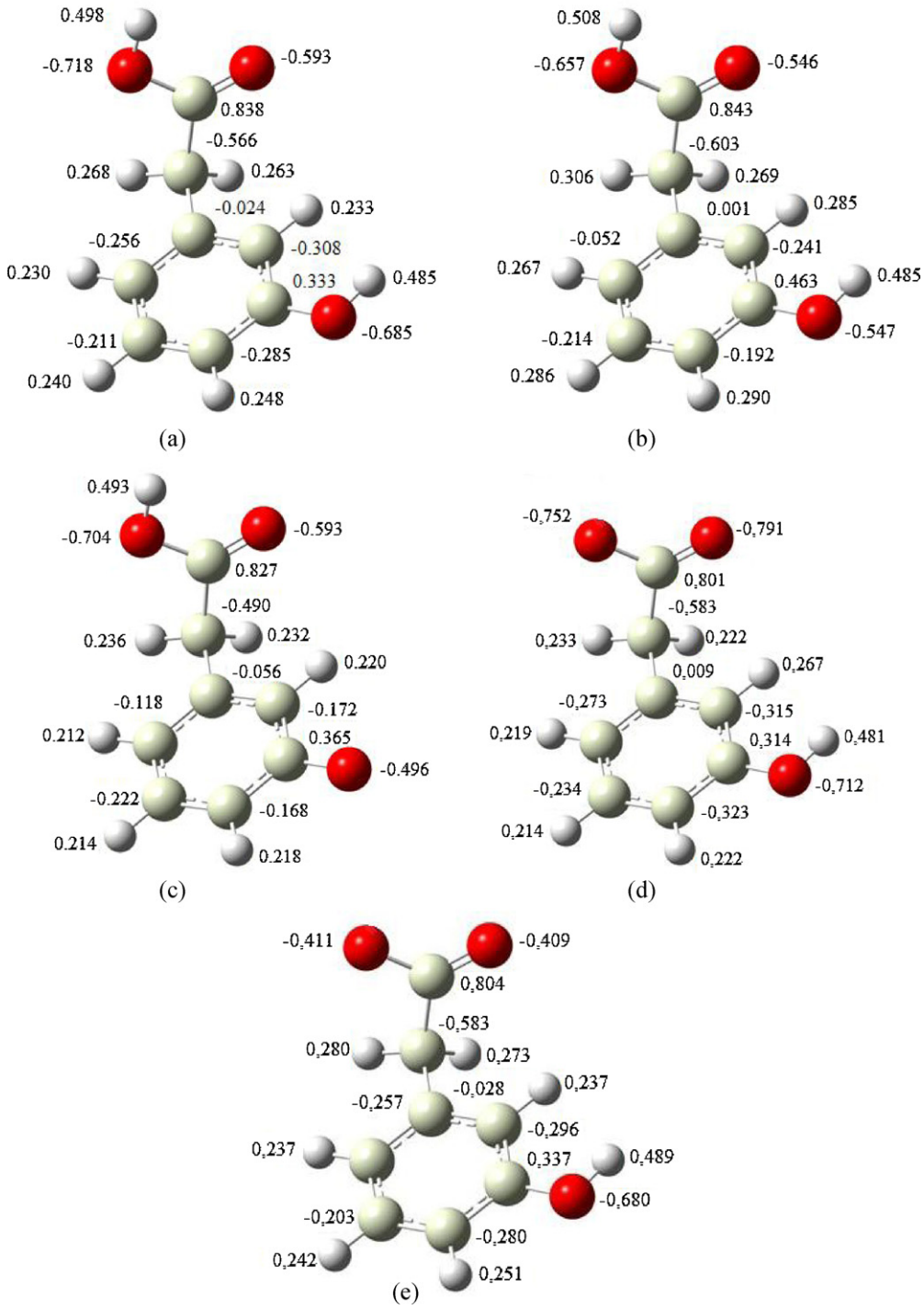

Fig. 2. Atomic charge distribution obtained using ChelpG for 3-HPA (a); 3-HPA-cr (b); 3-HPA-r (c); 3-HPAc (d); and 3-HPAc-r (e) [23].

substantially low. The same approximate trend is also observed for 3-HPA-r (Fig. 2c), a phenoxy radical.

In the electropolymerization, 3-HPA suffers a homolytic scission that results in free-radical species such as 3-HPA-cr or 3-HPA-r. The analysis of the partial atomic charges shows that carbon 6 suffers a considerable loss of electron density in both species, which suggests that this position is a potential reactive site for the electropolymerization.

For 3-HPAc (Fig. 2d), the oxygen atoms bonded to the carboxyl group exhibit a more negative partial charge, followed by the oxygen of the phenolic group. In this intermediate, carbon 7 also exhibits a negative charge greater than that observed for carbons 2, 4, 5 and 6. The lower partial charges over these carbons are probably a consequence of resonance effects in the aromatic ring. For 3-HPAc-r (Fig. 2e), the oxygen of the phenolic group is the atom with the most negative partial charge, followed by the oxygen atoms of the acetate group. The partial charges for the other atoms are similar to those estimated for 3-HPA.

A mean increase of 3.26° in the C(7)–C(8)–O(A) angle for the intermediates relative to that for 3-HPA is observed and can be related to the decrease in the C(7)–C(8) and C(8)–O(A) bond lengths. This decrease is confirmed by the bond-order analysis and by a

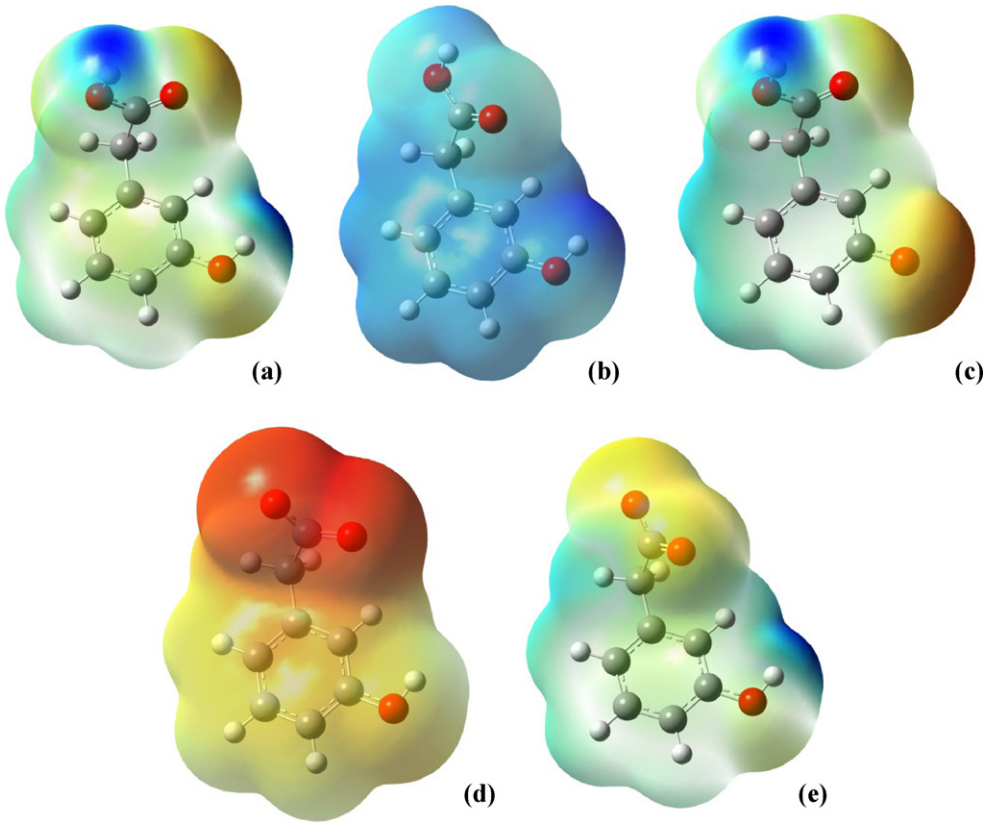

Fig. 3. Representation of the electron-density maps from total SCF density, mapped with the electrostatic potential (ESP) for 3-HPA (a); 3-HPA-cr (b); 3-HPA-r (c); 3-HPAc (d); and 3-HPAc-r (e).

substantial increase in the partial charge of the involved atoms. A 25% decrease in the C(1)–C(7)–C(8)–O(B) and C(6)–C(1)–C(7)–C(8) dihedral angles is observed in 3-HPAc compared to those in 3-HPA, which is caused by an increase in the electron density over the carboxylate group (Fig. 3). The carboxylate group suffers significant changes in the partial charges over the atoms that constitute these dihedrals, which also affects the bond orders.

The bond orders (Table 2) were calculated using the NBO method, and the atomic charges (Fig. 2) were calculated using ChelpG (charges from electrostatic potentials using a grid-based method) [23]. In this method, atomic charges are fitted to reproduce the molecular electrostatic potential at a number of points around the molecule. The charges calculated are frequently considered superior to the Mulliken charges because they depend much less on the underlying theoretical method used to compute the wave function (and thus the MEP) [24].

The electropolymerization of 3-HPA has been reported to occur efficiently under acid pH conditions over a graphite electrode surface and to be initiated by 3-HPA oxidation [19]. The electron transfer of 3-HPA to the electrode involves the formation of 3-HPA-cr (Fig. 3b), which loses a proton and gives rise to free-radical 3-HPA-r (Fig. 3c).

The electropolymerization of 3-HPA also can occur under neutral and alkaline pH conditions, although with very low yields, as indicated by the analysis of the cyclic voltammograms and reaction products [28]. Under neutral pH conditions, the initiation step is probably still based on 3-HPAc (Fig. 3d), which, when oxidized, gives rise to the 3-HPAc-r free radical (Fig. 3e). If the medium is strongly alkaline, the formation of the 3-phenoxy-acetate dianion (3-PAc^{2-}), a species with a high electron density in the whole structure (Fig. 4), is possible. The formation of 3-PAc^{2-} is suggested by the map of electron density from the total SCF density, which was mapped with the electrostatic potential (ESP) that was calculated using semi-empirical model RM1.

In an electron transfer to the graphite electrode, this species gives rise to the 3-phenoxide-acetate-anion radical ($3\text{-PAc}^{-\bullet}$), in which the electron density is concentrated on the carboxylate group (Fig. 5). However, the electron transfer from 3-PAc^{2-} should imply a considerable loss of electron density from the phenoxide group, which would affect the coupling between the intermediate species for the formation of the polymer and severely compromise the yield of the electropolymerization reaction [28].

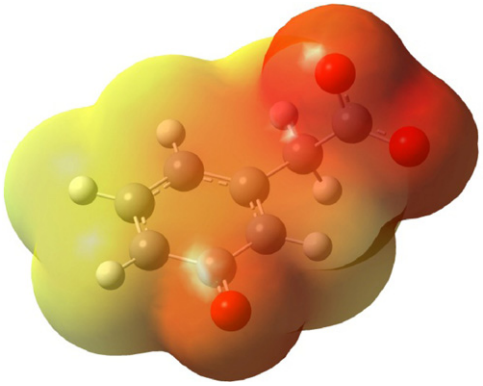

Fig. 4. Map of electron density from total SCF density mapped with the electrostatic potential (ESP) for the dianion 3-phenoxy-acetate (3-PAc^{2-}) and calculated using semi-empirical model RM1. The regions in red are richer in electron density and represent the carboxylate group and the semiquinone derived from deprotonation of phenolic OH. (For interpretation of the references to color in this figure legend, the reader is referred to the web version of the article.)

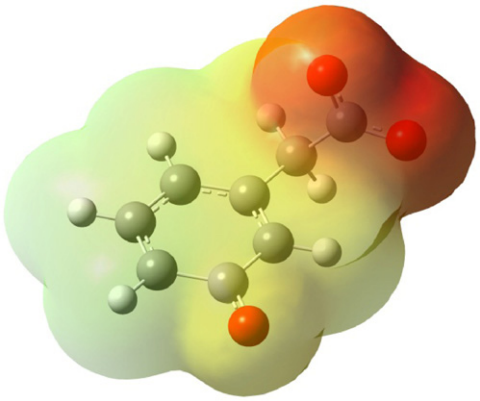

Fig. 5. Map of electron density from total SCF density mapped with the electrostatic potential (ESP) for the anion-radical 3-phenoxy-acetate (3-PAc$^{-\bullet}$) and calculated using semi-empirical model RM1. In this species, the electron density is concentrated on the carboxylate group.

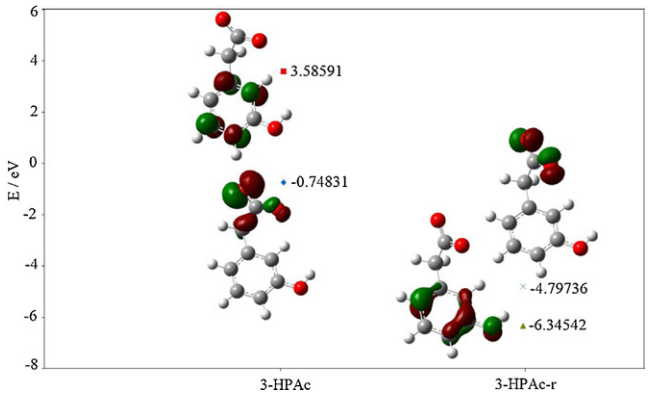

Fig. 7. Energy diagram of molecular orbitals (◆ HOMO, ■ LUMO, ▲ SOMO-α and X SOMO-β). 3-Hydroxyphenylacetate and the radical 3-hydroxyphenylacetate are represented on the *x*-axis in order from left to right. Each species has two eigenvalues, as shown in each column.

Figs. 6 and 7 present the energy diagram with the main frontier orbitals of 3-HPA and those of the intermediates involved in the electropolymerization. In these figures, the eigenvalues were expressed in electron volts. With the correlations between the frontier orbital energies, a better visualization of the interactions between the 3-HPA and the intermediates that should participate of the electropolymerization stages and result in the poly(3-HPA) is possible.

For 3-HPA and 3-HPA-cr, the frontier orbitals are located preferentially over the aromatic ring, whereas the SOMO of 3-HPA is located over the hydroxyl group and also over some positions in the aromatic ring, primarily on carbon 6. This result indicates a large electronic dispersion, which complicates any inference about the mechanism of electropolymerization. Although the state energy of the SOMO-α of 3-HPA-cr proves to be more compatible with the one associated with the HOMO of 3-HPA, the formation of free radicals in the electrochemical process favors the coupling between the SOMO-α of 3-HPA-r and the HOMO of the 3-HPA, which propagates the reaction. This coupling should preferably involve carbon 6 in 3-HPA, which is less sterically hindered and exhibits a greater tendency to acquire a less negative partial charge with the removal of an electron, and the unpaired electron located over the phenolic oxygen of the 3-HPA-r free radical.

In alkaline media, the ligand characteristic of the SOMO of 3-HPAc-r and the large energy difference between these molecular orbitals and the frontier orbitals of the deprotonated monomer is disadvantageous for the electropolymerization.

Data from electrochemical impedance measurements for a similar monomer, 4-hydroxyphenylacetic acid, suggest a direct relationship between the pH and the resistance to charge transfer, i.e., films with a large ohmic resistance to electron transfer tend to form as pH is increased [18]. From the quantum chemical point of view, the energy gap between the frontier orbitals of the probable structures formed under acidic pH (pH lower than pKa_1) is lower than the energy gap of frontier orbitals of the probable structures produced under neutral and alkaline pH (pH between pKa_1 and pKa_2). These results suggest a better efficiency for the electropolymerization under acidic conditions. According to the energy diagrams (Figs. 6 and 7), the small energy gap between the HOMO from 3-HPA and the SOMO-α from 3-HPA-r, which are probable structures under acidic pH conditions, is equal to 5.82×10^{-18} kJ. Among the orbitals related to the probable structures under neutral

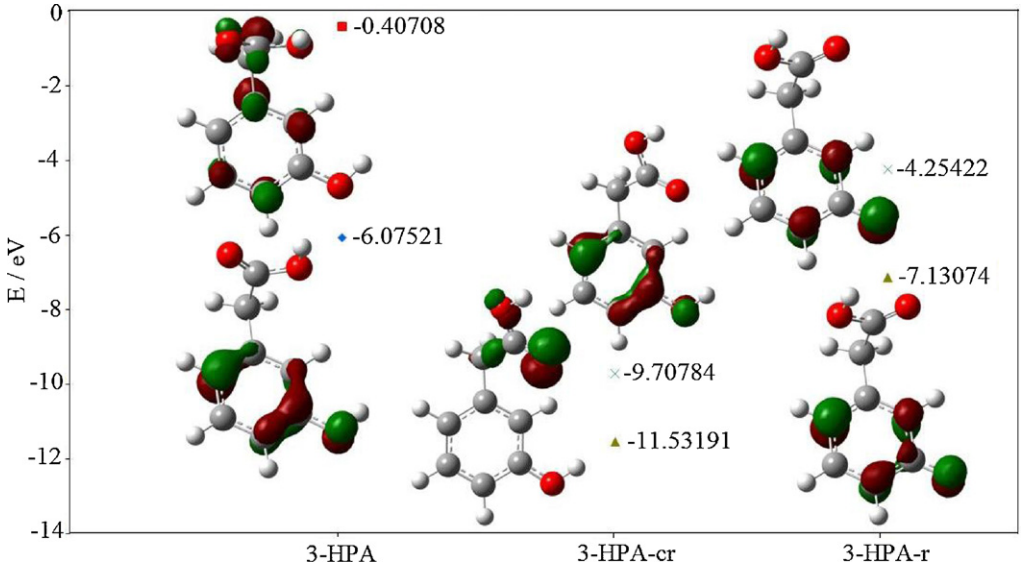

Fig. 6. Energy diagram of molecular orbitals (◆ HOMO, ■ LUMO, ▲ SOMO-α and X SOMO-β). 3-Hydroxyphenylacetic acid, its cation radical, and the radical 3-hydroxyphenylacetic are represented on the *x*-axis, in order from left or right. Each species presents two eigenvalues, as shown in each column.

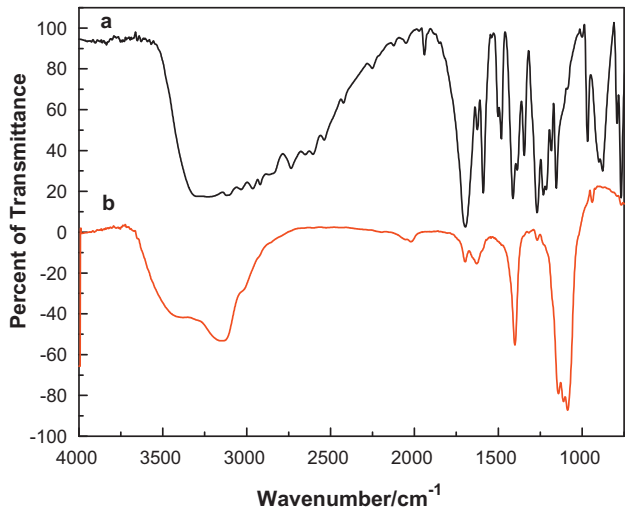

Fig. 8. FTIR spectra obtained from KBr pellets for (a) 3-HPA and (b) poly-(3-HPA), with 20 consecutive cycles, at a resolution of 4 cm^{-1}.

Table 3
Assignment of infrared signals for 3-HPA and poly-(3-HPA).

Wave number/cm^{-1}	Infrared signals for 3-HPA
3262	Band characteristic of axial deformation of O—H
1700	C=O axial deformation, characteristic of carboxylic acids
1577	Axial deformation C=C, typical of aromatic compounds
1468	Axial deformation C=C, typical of aromatic compounds
1391	C—O—H axial deformation, typical of phenolic compounds
1217	C—O axial deformation, typical of phenolic compounds
877	Out-of-plane angular deformation of aromatic C—H
714	Out-of-plane angular deformation of aromatic C—H
Wave number/cm^{-1}	**Infrared signals for poly-(3-HPA)**
3151	Angular out-of-plane deformation of aromatic O—H from carboxylic acids
1706	Low-intensity peak, characteristic of C=O axial deformation of carboxylic acids
1402	Axial deformation of aromatic C=C
1089	C—O—C asymmetric axial deformation, typical of ethers

pH conditions (HOMO from 3-HPAc and SOMO-β from 3-HPAc-r), the value is equal to 6.49×10^{-22} kJ.

The p*K*a values estimated for 3-HPA using the semi-empirical PM6 method show good agreement with experimental values. The theoretically estimated value of pKa_1 and pKa_2 were 0.03 and 0.11 p*K*a units lower, respectively, than the experimental values of 4.32 and 9.99.

Besides the low energy gap, another requirement for the intermolecular reaction is the symmetry between the involved frontier orbitals (most commonly HOMO and LUMO). The HOMO of 3-HPA exhibits characteristic ligand features that should favor the interaction with the SOMO-α of 3-HPA-r and result in radical-like reactions during the electropolymerization of poly(3-HPA).

The experimental infrared spectra of 3-HPA and poly(3-HPA) are presented in Fig. 8.

Table 3 presents the main characteristic bond deformations for these compounds. For the monomer (Fig. 8a), a large band related to the axial deformation of OH in carboxylic acids is observed at 3262 cm^{-1}. Additionally, the axial deformation of C=O of carboxylic acid can be seen at 1698 cm^{-1}. The theoretical spectra were corrected using a scale factor of 0.96, which has been recommended for the combination of the B3LYP hybrid functional and the 6-31G basis set [29].

A series of complex combinations of bands mostly related to deformations typical of aromatic compounds are observed. The bands at 1577 and 1468 cm^{-1} are related to axial deformations of aromatic C=C. At 1391 cm^{-1}, a C—O—H angular deformation occurs, which is typical for phenolic compounds. At 1217 cm^{-1}, a band related to C—O axial deformation, which is characteristic for phenolic compounds, and bands at 877 and 714 cm^{-1}, which are related to out-of-plane C—H angular deformations and are typical of aromatic compounds, are observed.

In contrast to the infrared spectrum of 3-HPA, the spectrum of poly(3-HPA) contains a smaller number of peaks related to the functional groups present in its structure. A band at 3149 cm^{-1} is observed, although with a different profile, which is characteristic of OH deformation of carboxylic acids. This band is accompanied by a shoulder at 3417 cm^{-1}, which suggests the presence of carboxylic groups in different positions within the polymer structure. The occurrence of a series of harmonic deformations is observed at 2026 cm^{-1} that are characteristic of tetra-substituted compounds. The existence of such harmonic distortions may be related to the occurrence of ring–ring bonds in positions 2 and 3 in poly(3-HPA). The band at 1706 and 1627 cm^{-1} are probably related to the axial deformation of C=O of carboxylic acids, which is consistent with the observed splitting in the band characteristic of OH deformation of carboxylic acid. As in 3-HPA, it is observed for poly-(3-HPA) axial deformations of aromatic C=C at 1399 cm^{-1}. Finally, at 1147 and 1086 cm^{-1} it is observed the superposition of three intense and defined bands related to C—O—C axial asymmetric deformation characteristic of ethers. The occurrence of this kind of deformation supports the proposition of the existence of ether groups in the polymer structure and suggests that the polymerization should involve the phenolic hydroxyl groups.

The evaluation of the results obtained in the present study allows us to propose a mechanism for the main route of the electropolymerization of 3-HPA (Scheme 2).

First, acidic medium is the most appropriate medium for the reaction. Protonated species at pH 0.5 tend to suffer oxidation, during which they release an electron to the electrode and a proton to the medium. This oxidation propagates the formation of polyether chains of 3-HPA because, being electronegative, the carboxyl group shifts the electron density, as evidenced by the partial charge on carbon 7 and the weakening of the OH bond of the phenolic group. The weakening of the OH bond ultimately benefits the homolytic cleavage of the phenolic hydrogen and leads to the formation of a phenoxy radical. In 3-HPA-cr, with respect to the electron-spin density, we highlight carbons C4 (0.112) and C6 (0.413), which show a higher probability of containing the unpaired electron on carbon 6 (reaction site). The remaining carbon atoms of the ring have zero spin density. Thus, carbon 6 is the most likely point of attack by the phenoxy radical because it is the atom that tends to become less negative when it loses an electron; this electron loss can be perceived by the variation in the partial charges of 3-HPA and the intermediates (Fig. 2). The coupling must occur between the SOMO-α of 3-HPA-r and the SOMO-β of 3-HPA-cr, which results in the ether bond observed in the IR spectra (Table 3). The propagation of the reaction should occur by pairing between the radicals formed from oxidation and deprotonation of the monomer and the cation radicals produced from the oxidation of the formed oligomers. The possibility of attack of the phenoxy radical on carbon 4 due to its position of low steric hindrance is also possible. However, this carbon should not exhibit a trend similar to that exhibited by carbon 6 to propagate the polymerization. Additionally, an attack by 3-HPA-cr in place of the phenoxy radical is less favorable in view of the non-pairing of the molecular orbitals involved and its positive electrostatic potential distributed throughout the structure.

Although the water absorption of the polymer makes a good-quality infrared spectrum difficult to obtain, strong signals in

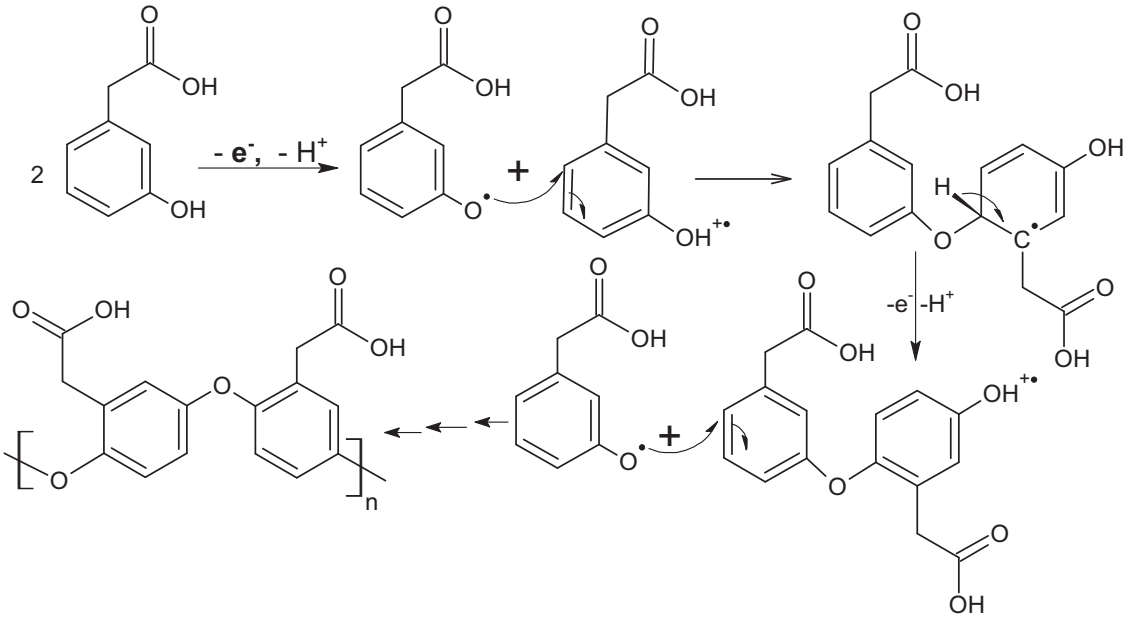

Scheme 2. Mechanism proposed for the formation of polyethers during the electropolymerization of 3-HPA in an acidic medium.

regions related to carboxylic groups proves its anionic characteristics. The relative ease with which the polymer absorbs water demonstrates its hygroscopic characteristics.

Importantly, an excessive number of oxidative cycles tend to significantly increase the surface area of the electrode, which may allow the occurrence of parallel polymerization by non-electrochemical routes and lead to the formation of polyesters.

The observations in this study allow us to also propose that the formation of polyesters should be favored in alkaline media because this reaction results in an extremely low yield [22]. The

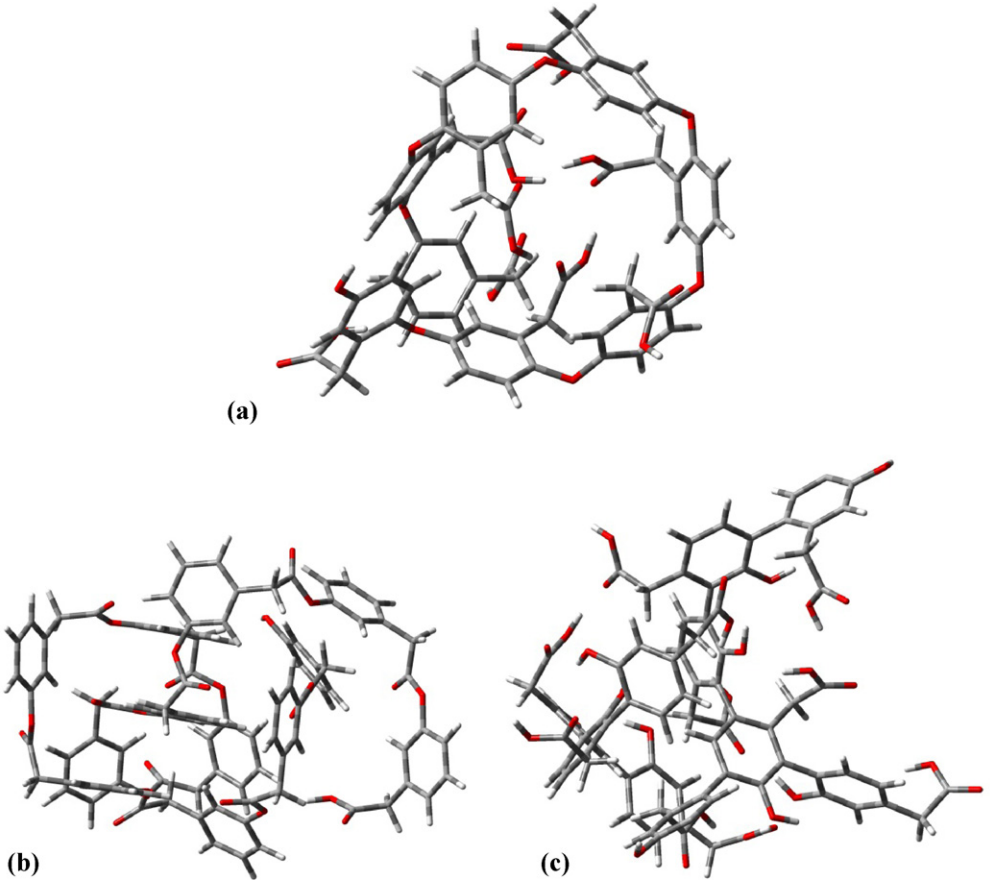

Fig. 9. Minimum-energy structures of the three octameric forms of species that should be part of the structure of the polymer produced from 3-HPA electropolymerization. These structures were optimized using DFT calculations: (a) 3-HPA-ether octamer, (b) 3-HPA-ester octamer, and (c) 3-HPA–C–C-bonded-rings octamer.

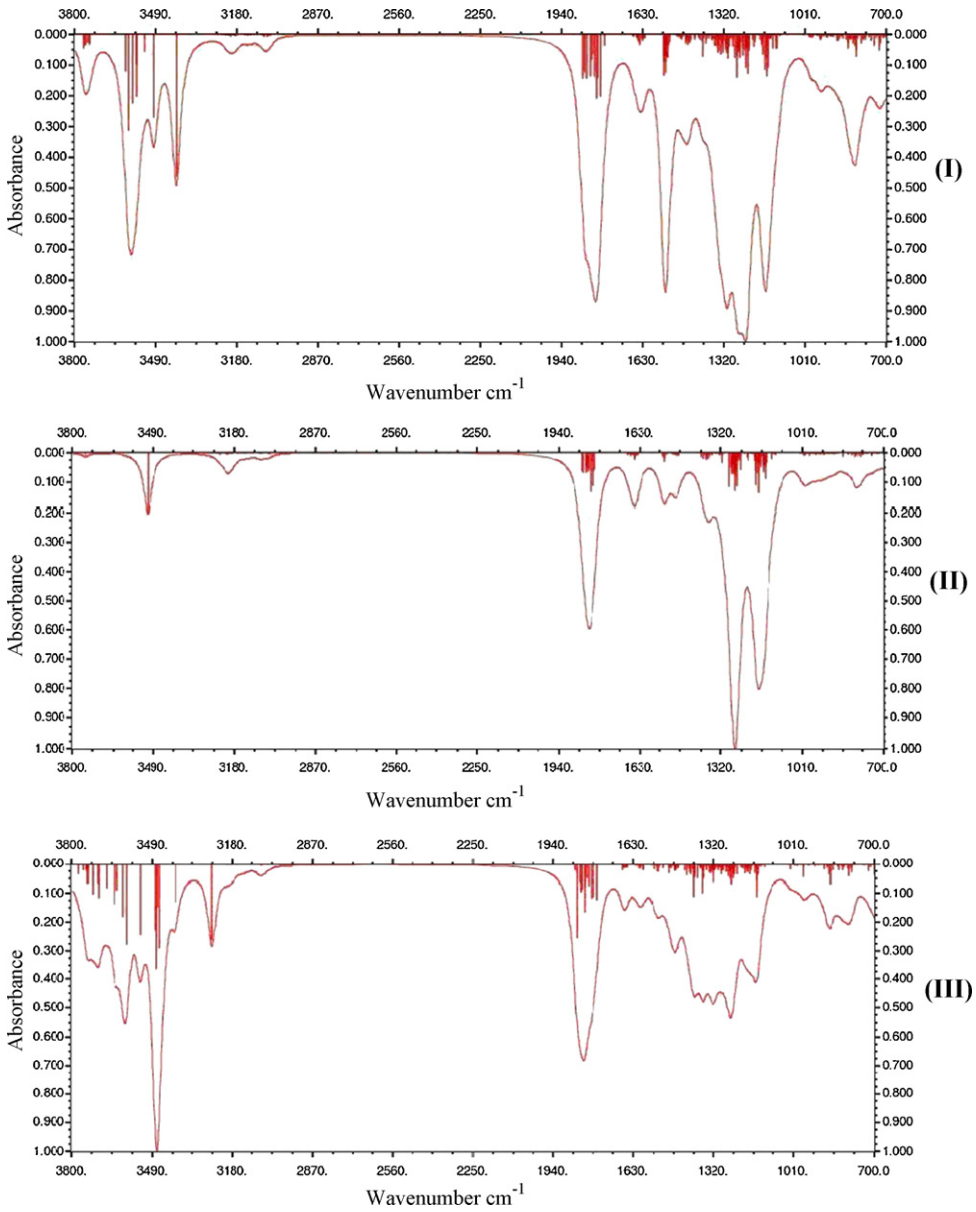

Fig. 10. Theoretical IR spectra simulated from DFT calculations for three possible octameric fragments formed during 3-HPA electropolymerization: (I) polyether; (II) bonded rings; and (III) polyester.

frontier orbitals of 3-HPAc and 3-HPAc-r suggest the occurrence of hyperconjugation involving carbon 7 with the deprotonated carboxyl group in its ligand HOMO feature. This carboxyl group should pair with the free-radical species whose SOMO-α is a ligand on the aromatic ring and with the phenolic hydroxyl, which allows the propagation of this reaction.

The different possible routes for electropolymerization lead us to propose a polymer that results from the combination of three different species formed from the coupling between the 3-HPA and the probable intermediates. The obtained global-minimum-energy structures of these species are presented in Fig. 9.

The theoretical IR spectra obtained for the octamers by full optimization followed by frequency calculations are shown in Fig. 10.

The attributions of the main vibrational frequencies for these models were compared with the experimental spectrum obtained for the polymer; the results are presented in Table 4.

The correlation between the theoretical and experimental results presented in Table 3 and 4 and the spectral profiles in Figs. 8 and 10 suggest the predominance of poly-(aryl ether) structures in the polymer obtained by electropolymerization. This agrees with the electroactive character of the polymer, indicating a conjugated structure. Despite the predominance of poly-(aryl ether) structures, during the diffusion of the monomeric active structures, other forms of coupling should occur, and so the polymer must present a complex structure, with polyester and poly-bonded ring-to-ring as possible components of the final structure.

Although the presented hypothesis should be consistent and suggests the most likely structure, other forms of pairing and nucleation were investigated for the polymerization of 3-HPA. Unlike the polymerization of aminophenol monomers studied under different pH conditions [30], we can assume in the formation of poly-(3-HPA), the occurrence of a competition between the electrochemical polymerization, with the formation of polyether or aromatic carbon–carbon pairs, and non-electrochemical reactions, with the formation of polyesters.

Table 4
Vibrational frequencies selected from theoretical IR spectra for three possible octameric fragments formed during 3-HPA electropolymerization compared to experimental data.

Selected vibrational frequencies of poly-3-HPA	EXP	Polyether		Polyester		Poly-bonded rings	
		B3LYP	RM1	B3LYP	RM1	B3LYP	RM1
Broad band characteristic of strain OH (carboxylic acids)	3151	3413 3581	2406 2537	–	–	3261	3061
Peak with low intensity characteristic of C=O deformation of carboxylic acids	1706	1794 1830	1813 1850	1807 1833	1973	1770	1970
Axial deformation of aromatic C=C	1402	1537	1412	1650	1439	1280	1244[a]
C—O—C asymmetric axial deformation, typical of ethers	1089	1346	1120	–	–	–	–

EXP: experimental values.
[a] Weak signal

4. Conclusions

In this study we investigated the formation of poly-(3-HPA) using cyclic voltammetry and theoretical calculations based on a combination of quantum mechanical and experimental results. The systematic analysis of the molecular orbitals of 3-HPA and the possible intermediates formed during the electropolymerization, as well as the comparison between the experimental FTIR spectra of the polymer and those of the theoretical models, suggest that the electropolymerization occurs predominantly through the formation of poly-(aryl ether) chains, in acid media. However, despite the predominance of poly-(aryl ether) structures, during the diffusion of the monomeric active structures, other forms of coupling should occur, and so the polymer must present a more complex structure, with polyester and poly-aromatic ring-to-ring pairs as possible components, in addition to poly-(aryl ether) in the final structure. Additionally, the occurrence of competition between electrochemical and non-electrochemical reactions implies in the coexistence of polyesters with the other possible structures.

A mechanism was proposed for the main reaction. The obtained structure opens the possibility to study the interactions between the polymer and biomolecules, which will certainly help advance research on electrochemical biosensors.

Acknowledgements

The authors thank CNPq, FAPEMIG and CAPES, Brazilian research agencies, for financial support and scholarships.

References

[1] H. Peng, L. Zhang, C. Soeller, J.T. Sejdic, Conducting polymers for electrochemical DNA sensing, Biomaterials 30 (2009) 2132–2148.
[2] Y. Wang, L. Yang, C. Yao, W. Qin, S. Yin, Enhanced performance and stability in polymer photovoltaic cells using lithium benzoate as cathode interfacial layer, Sol. Energy Mater. Sol. Cells 95 (2011) 1243–1247.
[3] H. Manjunatha, G.S. Suresh, Electrode materials for aqueous rechargeable lithium batteries, J. Solid State Electrochem. 15 (2011) 431–445.
[4] N.T. Kemp, R. Newbury, J.W. Cochrane, E. Dujardin, Electronic transport in conducting polymer nanowire array devices, Nanotechnology 22 (2011) 105202.
[5] R.M. Iost, W.C. Silva, J.M. Madurro, A.G. Brito-Madurro, L.F. Ferreira, F.N. Crespilho, Recent advances in nano-based electrochemical biosensors: application in diagnosis and monitoring of diseases, Front. Biosci. 3 (2011) 663–689.
[6] C. Malitesta, F. Palmisano, L. Torsi, P.G. Zambonin, Glucose fast-response amperometric sensor based on glucose oxidase immobilized in an electropolymerized poly(o-phenylenediamine) film, Anal. Chem. 62 (1990) 2735–2740.
[7] Y. Nakabayashi, M. Wakuda, H. Imai, Amperometric glucose sensors fabricated by electrochemical polymerization of phenols on carbon paste electrodes containing ferrocene as an electron transfer mediator, Anal. Sci. 14 (1998) 1069–1076.
[8] Y. Nakabayashi, H. Yoshikawa, Amperometric biosensors for sensing of hydrogen peroxide based on electron transfer between horseradish peroxidase and ferrocene as a mediator, Anal. Sci. 16 (2000) 609–613.
[9] S. Cosnier, Biosensors based on electropolymerized films: new trends, Anal. Bioanal. Chem. 377 (2003) 507–520.
[10] A.C. Pereira, A.S. Santos, L.T. Kubota, Trends in amperometric electrodes modification for electroanalytical applications, Quim. Nova 25 (2002) 1012–1021.
[11] M.O. Finot, M.T. McDermott, Characterization of n-alkanethiolate monolayers adsorbed to electrochemically deposited gold nanocrystals on glassy carbon electrodes, Electroanal. Chem. 488 (2000) 125–132.
[12] K. Nathalie, N.G. Guimard, C.E. Schmidt, Conducting polymers in biomedical engineering, Prog. Polym. Sci. 32 (2007) 876–921.
[13] L.R. Goulart, C.U. Vieira, A.P. Freschi, F.E. Capparelli, P.T. Fujimura, J.F. Almeida, L.F. Ferreira, I.M.B. Goulart, A.G. Brito-Madurro, J.M. Madurro, Biomarkers for serum diagnosis of infectious diseases and their potential application in novel sensor platforms, Crit. Rev. Immunol. 30 (2010) 201–222.
[14] L.F. Ferreira, J.F.C. Boodts, A.G.B. Madurro, J.M. Madurro, Gold electrodes modified with poly(4-aminophenol): incorporation of nitrogenated bases and an oligonucleotide, Polym. Int. 57 (2008) 644–650.
[15] C.M. Castro, S.N. Vieira, R.A. Gonçalves, A.G.B. Madurro, J.M. Madurro, Electrochemical and morphologic studies of nickel incorporation on graphite electrodes modified with polytyramine, J. Mater. Sci. 43 (2008) 475–482.
[16] F.B. Silva, S.N. Vieira, L.R. Goulart, J.F.C. Boodts, A.G.B. Madurro, J.M. Madurro, Electrochemical investigation of oligonucleotide-DNA hybridization on poly(4-methoxyphenethylamine), Int. J. Mol. Sci. 9 (2008) 1188–1195.
[17] L.F. Ferreira, L.M. Souza, D.L. Franco, A.C.H. Castro, A.A. Oliveira, J.F.C. Boodts, A.G. Brito-Madurro, J.M. Madurro, Formation of novel polymeric films derived from 4-hydroxybenzoic acid, Mater. Chem. Phys. 129 (2011) 46–52.
[18] T.A.R. Silva, L.F. Ferreira, J.F.C. Boodts, S.P. Eiras, J.M. Madurro, A.G.B. Madurro, Poly(4-hydroxyphenylacetic acid): a new material for immobilization of biomolecules, Polym. Eng. Sci. 48 (2008) 1963–1970.
[19] R.M.L. Oliveira, S.N. Vieira, H.C. Alves, E.G. França, D.L. Franco, L.F. Ferreira, A.G. Brito-Madurro, J.M. Madurro, Electrochemical and morphological studies of an electroactive material derived from 3-hydroxyphenylacetic acid: a new matrix for oligonucleotide hybridization, J. Mater. Sci. 45 (2010) 475–482.
[20] G.B. Rocha, R.O. Freire, A.M. Simas, J.J.P. Stewart, RM1: a reparameterization of AM1 for H, C, N, O, P, S, F, Cl, Br, and I, J. Comput. Chem. 27 (2006) 1101–1111.
[21] M.J. Frisch, G.W. Trucks, H.B. Schlegel, G.E. Scuseria, M.A. Robb, J.R. Cheeseman, G. Scalmani, V. Barone, B. Mennucci, G.A. Petersson, H. Nakatsuji, M. Caricato, X. Li, H.P. Hratchian, A.F. Izmaylov, J. Bloino, G. Zheng, J.L. Sonnenberg, M. Hada, M. Ehara, K. Toyota, R. Fukuda, J. Hasegawa, M. Ishida, T. Nakajima, Y. Honda, O. Kitao, H. Nakai, T. Vreven, J.A. Montgomery Jr., J.E. Peralta, F. Ogliaro, M. Bearpark, J.J. Heyd, E. Brothers, K.N. Kudin, V.N. Staroverov, R. Kobayashi, J. Normand, K. Raghavachari, A. Rendell, J.C. Burant, S.S. Iyengar, J. Tomasi, M. Cossi, N. Rega, J.M. Millam, M. Klene, J.E. Knox, J.B. Cross, V. Bakken, C. Adamo, J. Jaramillo, R. Gomperts, R.E. Stratmann, O. Yazyev, A.J. Austin, R. Cammi, C. Pomelli, J.W. Ochterski, R.L. Martin, K. Morokuma, V.G. Zakrzewski, G.A. Voth, P. Salvador, J.J. Dannenberg, S. Dapprich, A.D. Daniels, Ö. Farkas, J.B. Foresman, J.V. Ortiz, J. Cioslowski, D.J. Fox, Gaussian 09, Revision A.1, Gaussian, Inc., Wallingford, CT, 2009.
[22] J. Tomasi, B. Mennucci, R. Cammi, Quantum mechanical continuum solvation models, Chem. Rev. 105 (2005) 2999–3093.
[23] C.M. Breneman, K.B. Wiberg, Determining atom-centered monopoles from molecular electrostatic potentials. The need for high sampling density in formamide conformational analysis, J. Comput. Chem. 11 (1990) 361–373.
[24] C.J. Cramer, Essentials of Computational Chemistry: Theories and Models, 2nd ed., Wiley, 2004.
[25] J.J.P. Stewart, Optimization of parameters for semiempirical methods V: modification of NDDO approximations and application to 70 elements, J. Mol. Model. 13 (2007) 1173–1213.
[26] F. Mohammadi, N.G.J. Richards, W.C. Guida, R. Liskamp, M. Lipton, C. Caufield, G. Chang, T. Hendrickson, W.C. Still, MacroModel – an integrated software system for modeling organic and bioorganic molecules using molecular mechanics, J. Comput. Chem. 11 (1990) 440–467.
[27] A.R. Allouche, Gabedit: a graphical user interface for computational chemistry softwares, J. Comput. Chem. 32 (2010) 174–182.
[28] P.O. Martins, Synthesis, characterization and application of poly(3-hydroxyphenylacetic acid) in the development of a biosensor for detection of cardiac marker. Master's Thesis. Instituto de Química – UFU, 2011.
[29] Nist Standard Reference Database 101. http://cccbdb.nist.gov/.
[30] O. Abrahão Jr., T.S.P. Teixeira, J.M. Madurro, A.E.H. Machado, A.G. Brito-Madurro, J. Mol. Struct.: Theochem. 13 (2009) 28–37.